
F. Pioldi, R. Ferrari, E. Rizzi
"*A refined FDD algorithm for Operational Modal Analysis of buildings under earthquake loading*",
Proc. of the 26th International Conference on Noise and Vibration Engineering (ISMA2014),
Editors: P. Sas, D. Moens, H. Denayer,
KU Leuven, Belgium, September 15-17, 2014;
Book of Abstracts, p. 152;
CD-ROM Proceedings, ISBN 9789073802919,
Paper ID 593, p. 3353-3368 (16 pages).

# A refined FDD algorithm for Operational Modal Analysis of buildings under earthquake loading

**F. Pioldi** [1]**, R. Ferrari** [1]**, E. Rizzi** [1]
[1] Università di Bergamo, Dipartimento di Ingegneria (Dalmine)
viale G. Marconi 5, I-24044 Dalmine (BG), Italy
e-mail: **egidio.rizzi@unibg.it**

## Abstract
An autonomously-developed, refined Frequency Domain Decomposition (FDD) algorithm implemented within MATLAB is applied to the modal dynamic identification of civil frame buildings subjected to a set of strong ground motions. The performed research deals, as a necessary validation condition, with pseudo-experimental signals generated prior to the dynamic identification, from the numerical response of several shear-type frames. Strong motion modal parameters are then extracted and estimated successfully at given seismic input, taken as base excitation. Results turn-out very much consistent with targeted values, with quite limited errors in the modal parameter estimates, including for the modal damping ratios, ranging from low to high values. Notice that seismic excitation responses shall not fulfill traditional input assumptions of FDD techniques. This highlights the consistency of the present refined FDD algorithm in such a challenging framework. This paper shows that, in principle, a comprehensive modal dynamic identification of frame buildings through a refined FDD algorithm looks possible at seismic input.

## 1 Introduction

Operational Modal Analysis (OMA) techniques display two major advantages with respect to Experimental Modal Analysis (EMA) methods, including: no need of excitation devices; all (or part) of the measurements (coordinates) that may be used as references (i.e. input for the identification algorithm), so that the identification algorithm is of a Multi-Input-Multi-Output (MIMO) type [1], [2]. OMA procedures require only structural response signals induced by undetermined ambient loads (operating loads, wind, turbulence, traffic), in order to compute the corresponding Power Spectral Density (PSD) functions, from which it is possible to extract consistent estimates of the modal parameters [1].

The present work deals with the modal dynamic identification of shear-type frame structures by a refined Frequency Domain Decomposition (FDD) algorithm [3], implemented autonomously within MATLAB [4], [5], [6], [7]. FDD is a technique based on a spectral representation resting on the Singular Value Decomposition (SVD), and allows for estimating natural frequencies and mode shapes of the structural system [3]. A non-parametric technique for the estimate of modal damping ratios and undamped natural frequencies is also introduced with the Enhanced FDD (EFDD) [8]. A projection technique, called spatial decomposition, is then employed to estimate the modal coordinates in a different way: this method can remove some drawbacks of EFDD algorithms [9].

The FDD method should work properly within typical hypotheses such as stationary Gaussian white noise input, very lightly-damped structures and geometrically orthogonal mode shapes of close modes [3]. Hence, classical FDD formulations shall not be employed for non-stationary response signals such as seismic excitation responses and also for highly-damped structures [3], [6]. In the field of OMA, as opposed to different attempts that have already investigated the role of seismic response (output) signals in the Time Domain, such as [10], the analysis in the Frequency Domain seems to be lacking on that [11]. The present research developments attempt to address this issue [6], [7], [12], by considering strong motion input records used in a refined FDD algorithm, within a research scenario that looks actually challenging in the present dedicated literature.

In this paper, pseudo-experimental response signals generated prior to the dynamic identification (by direct time integration from a set of given earthquake recordings, taken as base excitation) are adopted as input channels for the developed FDD algorithm. Despite that strong motion records should not fit among the canonical excitation input of FDD techniques, the present results turn-out very much consistent on the expected target values, with quite limited errors in the modal parameter estimates. Through the identification results of a series of eight different strong ground motions applied as base excitation to shear-type frame structures, this paper shows that, in principle, the FDD dynamic identification of modal parameters shall be possible at seismic input. Some key issues for the dynamic identification are also originally treated and discussed, either here or within separate dedicated attempts [5], [6], [7], [12].

Subsequent Section 2 outlines the theoretical fundamentals of FDD techniques and, starting from the latter, shows the basic features of the developed refined FDD algorithm. Section 3 presents the characteristics of eight strong ground motions used as base excitation for the frame structures. Section 4 outlines comprehensive results on the modal dynamic identification at seismic input, considering specifically a six-storey shear-type frame. Main conclusions are finally gathered in Section 5.

# 2 Fundamentals of FDD techniques

The common feature of Frequency Domain Decomposition methods is the evaluation of the PSD functions of the structural system responses. FDD methods operate then a SVD at each line of the frequency spectrum, separating noisy data from disturbances of various source [1]. The PSD matrix is thus decomposed into a set of auto-spectral density functions, each corresponding to a SDOF system, from which natural frequencies and mode shapes can be estimated [3]. If classical FDD assumptions are not satisfied, the SVD may result approximated, leading to noisy or untreatable results. However, in the present section original arrangements and strategies used by the proposed algorithm [4], [5] are shown, leading to very good modal parameter estimates, as outlined in [12].

## 2.1 Modal decomposition of the PSD matrix

The FDD theory is based on the typical input/output relationship of a general stationary random process for a MDOF system [9], [13]:

$$\mathbf{G}_{yy}(\omega) = \overline{\mathbf{H}}(\omega)\mathbf{G}_{xx}(\omega)\mathbf{H}^{T}(\omega) \tag{1}$$

where $\mathbf{G}_{xx}(\omega)$ is the (r × r) PSD matrix of the input, r being the number of input channels (references), $\mathbf{G}_{yy}(\omega)$ is the (m × m) PSD matrix of the output, m being the number of output signals (responses or measurements), $\mathbf{H}(\omega)$ is the (m × r) Frequency Response Function (FRF) matrix; the overbar denotes complex conjugate and symbol T transpose. Both $\mathbf{G}_{xx}(\omega)$ and $\mathbf{G}_{yy}(\omega)$ matrices derive from Finite Fourier Transforms for the PSD evaluation, see for details [5], [13].

Also, the FRF $\mathbf{H}(\omega)$ may be written in pole/residue form [13]:

$$\mathbf{H}(\omega) = \sum_{k=1}^{n} \frac{\mathbf{R}_k}{i\,\omega - \lambda_k} + \frac{\overline{\mathbf{R}}_k}{i\,\omega - \overline{\lambda}_k} \tag{2}$$

where n is the number of modes of vibration, $\lambda_k$ and $\overline{\lambda}_k$ are the poles (in complex conjugate pairs) of the FRF function [5], and $\mathbf{R}_k$ the (m × r) residue matrix, that can be expressed as [3], [5]:

$$\mathbf{R}_k = \boldsymbol{\phi}_k \boldsymbol{\Gamma}_k^{T} \tag{3}$$

where $\boldsymbol{\phi}_k = [\ \phi_{k1}\ \ \phi_{k2}\ \ \ldots\ \ \phi_{km}\ ]^T$ and $\boldsymbol{\Gamma}_k = [\ \Gamma_{k1}\ \ \Gamma_{k2}\ \ \ldots\ \ \Gamma_{kr}\ ]^T$ are the $k^{th}$ (m × 1) mode shape vector and (r × 1) modal participation factor vector, respectively [5]. Then, when all output measurements are taken as input references (i.e. when m = r), $\mathbf{H}(\omega)$ becomes a square matrix. Then, Eq. (1), through Eq. (2), can be rewritten as [5], [6], [12]:

$$\mathbf{G}_{yy}(\omega) = \sum_{k=1}^{n}\sum_{s=1}^{n}\left(\frac{\overline{\mathbf{R}}_k G_{xx}}{-i\omega-\overline{\lambda}_k} + \frac{\mathbf{R}_k G_{xx}}{-i\omega-\lambda_k}\right)\left(\frac{\mathbf{R}_s^T}{i\omega-\lambda_s} + \frac{\mathbf{R}_s^H}{i\omega-\overline{\lambda}_s}\right) \tag{4}$$

where hermitian symbol H denotes complex conjugate and transpose. This formulation is possible using the fact that the PSD matrix $\mathbf{G}_{xx}(\omega)$ *is constant for a stationary zero mean white noise input* and its representation degenerates to a single scalar constant $G_{xx}$ [13]; due to this fact and remembering the formulations of the PSD matrices by Short Time Fourier Transforms [13], the PSD matrix $\mathbf{G}_{xx}(\omega)$ is also real-valued and non-negative, so that $\mathbf{G}_{xx}(\omega) \Rightarrow G_{xx} = \overline{G}_{xx}$. Thus, by remembering the properties of $\mathbf{G}_{xx}(\omega)$ and by applying the Heaviside partial fraction expansion theorem to Eq. (4), one can obtain the final reduced pole/residue form for the output PSD matrix as follows [3], [9]:

$$\mathbf{G}_{yy}(\omega) = \sum_{k=1}^{n} \frac{\mathbf{A}_k}{i\omega-\lambda_k} + \frac{\mathbf{A}_k^H}{-i\omega-\overline{\lambda}_k} + \frac{\overline{\mathbf{A}}_k}{i\omega-\overline{\lambda}_k} + \frac{\mathbf{A}_k^T}{-i\omega-\lambda_k} \tag{5}$$

where $\mathbf{A}_k$ is the residue matrix of the PSD output corresponding to the k$^{th}$ pole $\lambda_k$. As for the PSD output itself, the residue matrix is an (m × m) hermitian matrix given by [9]:

$$\mathbf{A}_k = \sum_{s=1}^{n}\left(\frac{\mathbf{R}_s}{-\lambda_k-\lambda_s} + \frac{\overline{\mathbf{R}}_s}{-\lambda_k-\overline{\lambda}_s}\right) G_{xx}\mathbf{R}_k^T \tag{6}$$

*For light inherent structural damping* (small damping ratios $\zeta_k \ll 1$), the pole can be expressed in an approximate form [5], [6]; then, in the vicinity of the k$^{th}$ modal frequency, only the $\overline{\mathbf{R}}_k$ term survives, so that the residue matrix can be derived approximately from Eq. (6) as [9]:

$$\mathbf{A}_k \simeq \frac{\overline{\mathbf{R}}_k G_{xx}\mathbf{R}_k^T}{2\zeta_k\omega_k} = \frac{\overline{\boldsymbol{\phi}}_k \boldsymbol{\Gamma}_k^H G_{xx}\boldsymbol{\Gamma}_k \boldsymbol{\phi}_k^T}{2\zeta_k\omega_k} = d_k\overline{\boldsymbol{\phi}}_k\boldsymbol{\phi}_k^T \tag{7}$$

where $\zeta_k$ are the modal damping ratios (index k spans the modes, k = 1, …, n) and the term:

$$d_k = \frac{\boldsymbol{\Gamma}_k^H G_{xx}\boldsymbol{\Gamma}_k}{2\zeta_k\omega_k} \tag{8}$$

is a real scalar. Then, with the formulation of Eq. (7), the residue matrix $\mathbf{A}_k$ becomes proportional to a matrix based on the mode shape vector, i.e. $\mathbf{A}_k \propto \overline{\mathbf{R}}_k G_{xx}\mathbf{R}_k^T = \overline{\boldsymbol{\phi}}_k \boldsymbol{\Gamma}_k^H G_{xx}\boldsymbol{\Gamma}_k\boldsymbol{\phi}_k^T \propto d_k\,\overline{\boldsymbol{\phi}}_k\boldsymbol{\phi}_k^T$. So, by substituting Eq. (7) into Eq. (5) one gets:

$$\mathbf{G}_{yy}(\omega) = \sum_{k=1}^{n} \frac{d_k\overline{\boldsymbol{\phi}}_k\boldsymbol{\phi}_k^T}{i\omega-\lambda_k} + \frac{d_k\overline{\boldsymbol{\phi}}_k\boldsymbol{\phi}_k^T}{-i\omega-\overline{\lambda}_k} + \frac{d_k\boldsymbol{\phi}_k\boldsymbol{\phi}_k^H}{i\omega-\overline{\lambda}_k} + \frac{d_k\boldsymbol{\phi}_k\boldsymbol{\phi}_k^H}{-i\omega-\lambda_k} \tag{9}$$

In the narrow band with spectrum lines in the vicinity of a modal frequency, only the first two terms in Eq. (9) are dominant, since their denominator terms become smaller than to the other two [5], [6]. Taking this into account, the previous equation can be simplified as:

$$\mathbf{G}_{yy}(\omega) \simeq \sum_{k=1}^{n} \frac{d_k\overline{\boldsymbol{\phi}}_k\boldsymbol{\phi}_k^T}{i\omega-\lambda_k} + \frac{d_k\overline{\boldsymbol{\phi}}_k\boldsymbol{\phi}_k^T}{-i\omega-\overline{\lambda}_k} = \overline{\boldsymbol{\Phi}}\left\{\mathrm{diag}\left[\Re e\left(\frac{2d_k}{i\omega-\lambda_k}\right)\right]\right\}\boldsymbol{\Phi}^T \tag{10}$$

where $\boldsymbol{\Phi}$ is the eigenvector matrix, $\boldsymbol{\Phi} = [\,\boldsymbol{\phi}_1 \;\; \boldsymbol{\phi}_2 \;\; \dots \;\; \boldsymbol{\phi}_n\,]$, gathering all eigenvectors $\boldsymbol{\phi}_i$ as columns. Eq. (10) represents a modal decomposition of the output PSD matrix. The contribution to the spectral density matrix from a single mode k can be expressed as:

$$\mathbf{G}_{yy}(\omega_k) \simeq \overline{\boldsymbol{\phi}}_k\left\{\mathrm{diag}\left[\Re e\left(\frac{2d_k}{i\omega-\lambda_k}\right)\right]\right\}\boldsymbol{\phi}_k^T \tag{11}$$

The final form of the $\mathbf{G}_{yy}(\omega_k)$ matrix in Eq. (11) is then decomposed, using the SVD technique, as explained later, into a set of singular values and corresponding singular vectors. From the former, natural frequencies are extracted; from the latter, approximate mode shapes are obtained.

## 2.2 Modal dynamic identification by a refined FDD technique

The response of the structure $\mathbf{y}(t)$ can be expressed in terms of modal coordinates:

$$\mathbf{y}(t) = \sum_{k=1}^{n} \boldsymbol{\phi}_k \mathrm{p}_k(t) = \boldsymbol{\Phi}\mathbf{p}(t) \tag{12}$$

where $\mathbf{p}(t)$ is the vector of principal coordinates $\mathrm{p}_k(t)$. The response signals (input signals for the algorithm; e.g. accelerations, as considered here) shall be correlated, with the purpose of obtaining the matrix of the auto- and cross-correlation functions in the time domain, $\mathbf{R}_{yy}(\tau)$, a starting point of the developed FDD algorithm [9]:

$$\mathbf{R}_{yy}(\tau) = \mathrm{E}\left[\bar{\mathbf{y}}(t+\tau)\mathbf{y}(t)^{\mathrm{T}}\right] = \lim_{T\to\infty}\frac{1}{T}\int_{-T/2}^{T/2}\bar{\mathbf{y}}(t+\tau)\mathbf{y}(t)^{\mathrm{T}}\,\mathrm{d}t = \mathrm{E}\left[\bar{\boldsymbol{\Phi}}\,\bar{\mathbf{p}}(t+\tau)\mathbf{p}(t)^{\mathrm{T}}\boldsymbol{\Phi}^{\mathrm{T}}\right] = \bar{\boldsymbol{\Phi}}\,\mathbf{R}_{pp}(\tau)\boldsymbol{\Phi}^{\mathrm{T}} \tag{13}$$

where $\mathbf{R}_{pp}(\tau) = \mathrm{E}\,[\,\bar{\mathbf{p}}(t+\tau)\,\mathbf{p}(t)^{\mathrm{T}}\,]$ is the auto- and cross-correlations response matrix (in principal coordinates) and E denotes the expected value (calculated numerically in proper ways, see e.g. [12], [13]).

In the presence of noisy or weakly-stationary data (or non-stationary data, as the earthquakes treated in this work), the $\mathbf{R}_{yy}(\tau)$ matrix can be further processed to obtain an untrended (and unbiased) well-defined version. This expedient may lead to a refinement of the subsequent estimates, as extensively described in [12]. The auto- and cross-correlation functions of Eq. (13) are then transformed into the frequency domain by Discrete Fourier Transform (Fast Fourier Transform, FFT, classical Cooley-Tukey procedure), to obtain the PSD matrix of the responses, $\mathbf{G}_{yy}(\omega)$:

$$\mathbf{G}_{yy}(\omega) = \Im\left[\mathbf{R}_{yy}(\tau)\right] = \Im\left[\bar{\boldsymbol{\Phi}}\,\mathbf{R}_{pp}(\tau)\boldsymbol{\Phi}^{\mathrm{T}}\right] = \bar{\boldsymbol{\Phi}}\,\mathbf{G}_{pp}(\omega)\boldsymbol{\Phi}^{\mathrm{T}} \tag{14}$$

where $\mathbf{G}_{pp}(\omega) = \Im\,[\mathbf{R}_{pp}(\tau)]$ is the PSD matrix of the responses (in principal coordinates); this makes clearly visible the close relationship between the modal decomposition of Eq. (10) and Eq. (14).

Rather than steps from Eq. (12) to Eq. (14), another common way to obtain an estimate of the PSD matrix of responses, $\mathbf{G}_{yy}(\omega)$, is the so-called Welch Modified Periodogram method [12], [14]. The present refined FDD algorithm displays the powerful feature of implementing both methods. According to the characteristics of the recorded structural responses, this may effectively help in the estimates [12]. Now, as it is common in stochastic dynamics [9], [13], it is possible to assume that the modal coordinates are un-correlated; thanks to this assumption, the cross-correlation functions of the response vanish, so that the $\mathbf{R}_{pp}(\tau)$ and $\mathbf{G}_{yy}(\omega)$ matrices are assumed to be diagonal. Then, if the mode shapes (the columns of matrix $\boldsymbol{\Phi}$) are orthogonal to each other, Eq. (14) represents a spectral decomposition:

$$\mathbf{G}_{yy}(\omega) = \sum_{k=1}^{n} \mathrm{G}_k(\omega)\bar{\boldsymbol{\phi}}_k\boldsymbol{\phi}_k^{\mathrm{T}} \tag{15}$$

where $\mathrm{G}_k(\omega)$ is the auto-spectral density function of the $k^{th}$ modal coordinate. Then, remembering Eqs. (10) and (14), it is possible to consider the SVD of the transpose of the response PSD matrix:

$$\mathbf{G}_{yy}^{\mathrm{T}}(\omega) \simeq \boldsymbol{\Phi}\left\{\mathrm{diag}\left[\Re\mathrm{e}\left(\frac{2\mathrm{d}_k}{\mathrm{i}\,\omega-\lambda_k}\right)\right]\right\}\boldsymbol{\Phi}^{\mathrm{H}} = \mathbf{USU}^{\mathrm{H}} \tag{16}$$

where $\mathbf{U}$ is a unitary complex matrix (i.e. $\mathbf{UU}^{\mathrm{H}} = \mathbf{U}^{\mathrm{H}}\mathbf{U} = \mathbf{I}$) holding the singular vectors (i.e. the eigenvectors) and $\mathbf{S}$ is a real diagonal matrix holding the singular values (i.e. the eigenvalues). In general, the SVD of an arbitrary matrix $\mathbf{A}$ is given by [2], [13]:

$$\mathbf{A} = \mathbf{USV}^{\mathrm{H}} \tag{17}$$

where $\mathbf{U}$ and $\mathbf{V}$ are unitary matrices holding the left and right singular vectors and $\mathbf{S}$ is a rectangular matrix holding the non-zero singular values. Remembering that PSD matrix $\mathbf{G}_{yy}(\omega)$ is Hermitian, namely $\mathbf{G}_{yy}^{\mathrm{H}}(\omega) = \mathbf{G}_{yy}(\omega)$, one has $\mathbf{G}_{yy}^{\mathrm{T}}(\omega) = \mathbf{USV}^{\mathrm{H}} = \mathbf{VSU}^{\mathrm{H}}$. However, this does not imply that $\mathbf{U} = \mathbf{V}$. Since all PSD matrices embed energy content, they are positive definite [13]; then, $\mathbf{U} = \mathbf{V}$ and the SVD of a PSD matrix can always be expressed by Eq. (16), factorization also known as spectral theorem [9], [13].

The above-mentioned SVD technique is performed at each frequency line $\omega = \omega_i$. Then, from Eq. (16) it is possible to obtain, at the discrete frequencies $\omega_i$:

$$\mathbf{G}_{yy}^{T}(\omega_i) = \mathbf{U}_i \mathbf{S}_i \mathbf{U}_i^{H} \tag{18}$$

where, at frequency line $\omega_i$, $\mathbf{U}_i$ is the matrix of the n singular vectors $\mathbf{u}_{ij}$ and $\mathbf{S}_i$ is the diagonal matrix containing the n singular values $s_{ij}$, with $j = 1, \ldots, n$. Starting from the SVD of Eq. (18), modal identification can be made around a modal peak in the frequency domain, that can be located by a peak-picking procedure on the plot of the singular values. This is typically shown in Fig. 1a. The previous peak-picking procedure can be applied also to the SV product plot, as originally treated in [5]. This feature may support the peak-picking in case of very high damping or noisy data, and improve estimation results. Especially, when only the $k^{th}$ principal value is dominant, i.e. it reaches the maximum near the modal frequency $\omega_k$, the response PSD matrix can be approximated by a unitary rank matrix [3]:

$$\mathbf{G}_{yy}^{T}(\omega_i = \omega_k) \simeq s_k \mathbf{u}_{k1} \mathbf{u}_{k1}^{H} \tag{19}$$

where the first singular value at the $k^{th}$ resonance frequency provides an estimate, with unitary normalization, of the related mode shape:

$$\hat{\boldsymbol{\phi}}_k = \mathbf{u}_{k1} \tag{20}$$

The identified mode shape is then compared to the others in its proximity [3]; this allows to nearby investigate the dominant mode: in fact, if the mode is effectively dominant, the mode shape for that interval does not vary. It is possible to assess this by making base reference to the MAC (Modal Assurance Criterion) index:

$$\mathrm{MAC}(\boldsymbol{\phi}_r, \boldsymbol{\phi}_s) = \frac{\left|\boldsymbol{\phi}_r^{H} \boldsymbol{\phi}_s\right|^2}{\left|\boldsymbol{\phi}_r^{H} \boldsymbol{\phi}_r\right| \left|\boldsymbol{\phi}_s^{H} \boldsymbol{\phi}_s\right|} \tag{21}$$

The MAC index represents a sort of square of the correlation between two modal vectors $\boldsymbol{\phi}_r$, $\boldsymbol{\phi}_s$. If the MAC index is 1, the two compared vectors can be considered identical; if 0, clearly distinct (orthogonal). As long as a principal vector related to a frequency around the modal peak displays a high MAC value (near 1, say larger than 0.8÷0.9), related to the estimated mode shape, the corresponding principal value locates a subset of SV that belongs to the SDOF density function [3], [9]. Further indices based on MAC formula (21) are also used below in Section 4, to assess the validity of the estimated mode shapes.

### 2.2.1 Estimate of the modal damping ratios

After the estimations of natural damped frequencies and mode shapes, it is possible to evaluate modal damping ratios and undamped natural frequencies, according to the main steps of the EFDD technique [8]. The singular value of the estimated mode shape represents the power spectral density function of the corresponding SDOF system [8]. Thus, the developed refined FDD algorithm has been implemented according to the main phases below.

The SDOF power spectral density function is identified around the $k^{th}$ resonance peak, by comparing the associated estimated mode shape to those at the frequency lines in its proximity, in terms of MAC filtering, with a level of confidence set first to 0.9 [3]. This phase is usually referred to as spectral bell identification. A sample of such procedure is shown in Fig. 1b. Then, an estimate of the SDOF correlation function (related to the resonance peak) should be obtained by taking back the previous subset of singular values to the time domain, by using an Inverse Discrete Fourier Transform (IDFT) algorithm. In this process, remaining parts of the PSD function that lay outside the frequency window of the spectral bell are simply reset to zero [4], [5].

The antitransformed signal is normalized, by dividing it by its maximum value. All the extrema, i.e. peaks and valleys, that shall represent the free decay of a damped SDOF system, are identified in an appropriate time window, as it can be seen in Fig. 2a. The first two peaks and valleys (at least) must be excluded. Indeed, they may induce errors in subsequent operations [8], [12]. The selection of the correct time window represents the most difficult part of the operation and may require a refined loop algorithm, as outlined below. Jointly to the spectral bell identification, these operations derive from truncated data and might introduce bias errors in the damping estimates. This disadvantage must be taken into account especially with closely-spaced modes [5]. An inspection about content, decimation and frequency resolution must be necessary, to reach crystal-clear time window representations [5].

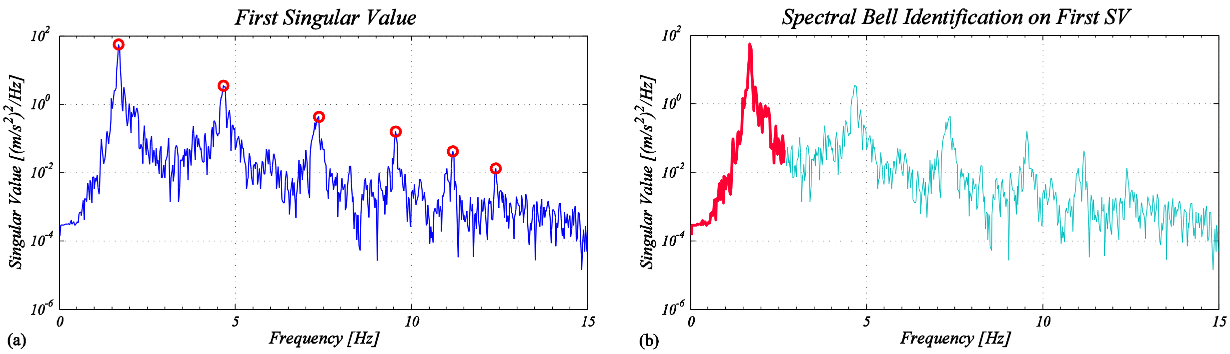


Figure 1: Display of the peak picking technique on the first singular value and of the spectral bell identification of the first mode; six-storey frame, El Centro earthquake.

Through picking of both peaks and valleys in the selected time window, it is possible to assess the logarithmic decrement δ:

$$\delta = \frac{2}{k} \ln\left(\frac{r_0}{|r_k|}\right) \tag{22}$$

where k is an integer index counter of the $k^{th}$ extreme of the auto-correlation function, k = 1, 2, …, while $r_0$ and $r_k$ are the initial and the $k^{th}$ extreme value of the auto-correlation function, respectively. Then, a linear relation can be obtained in terms of counter k [5], [8]:

$$2\ln\left(|r_k|\right) = 2\ln\left(r_0\right) - \delta k \tag{23}$$

which can be plotted and fitted with a straight line (see a sample in Fig. 2b). The logarithmic decrement δ is then estimated by the slope of this straight line, through linear regression on k and 2 ln($|r_k|$). The correct outcome of this linear regression operation is directly connected to the adequacy of the time window selection. These two steps, jointly with the earlier choice of the spectral bell, must be performed by an iterative operation of advanced optimization: if the linear fit does not produce adequate results (e.g. there are few and noisy points), the time window is recalibrated and regression is reperformed, until when a reliable estimate of δ is obtained, see flow chart in [5]. Also, the MAC index setting to perform spectral bell identification is fine-tuned, with the aim of developing the clearest possible antitransformed time signal. Such a double-iterative procedure is implemented in the present FDD algorithm and leads to quite accurate estimates of the modal damping ratios.

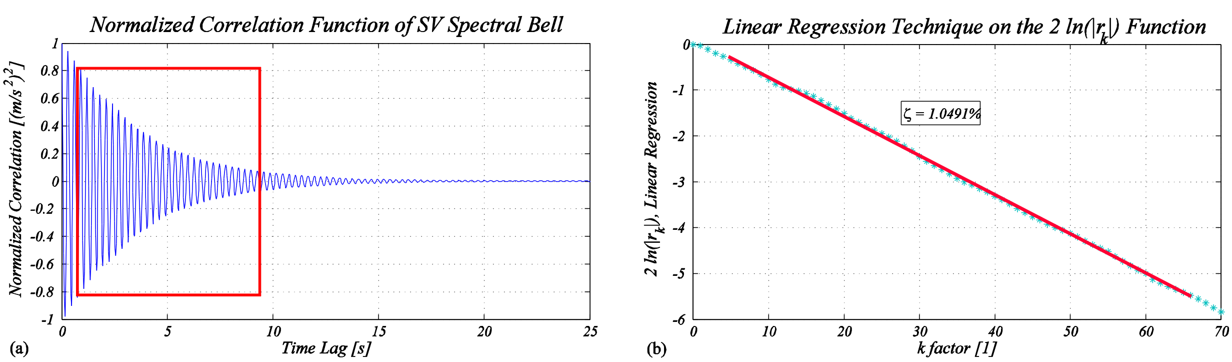


Figure 2: Selected time window of the normalized IDFT and linear regression technique for the estimate of the modal damping ratio; first mode, six-storey frame, El Centro earthquake.

Another important issue related to the damping ratio estimation belongs to the frequency resolution adopted during the PSD matrix evaluation. The use of a correct frequency resolution during computations affects directly the number of points which can be used during the linear regression (and consequently the reliability of results) [5], [12]. Especially with short structural recordings (e.g. acquisitions derived from earthquakes), the frequency resolution may be enhanced by increasing the number of points used for the PSD matrix computations. This can be done by adding a zero-excitation time window at the end of the recordings, thus increasing the length of the recordings with an operation that is known as zero-padding in classical signal analysis [5], [13]. This issue is fundamental to improve the outcomes of the damping ratio estimates; also, the estimates of the other modal parameters (i.e. natural frequencies and mode shapes) are coherently improved [12]. Finally, from the estimated logarithmic decrement $\delta = \delta_k$ of mode k the corresponding modal damping ratio $\zeta_k$ can be classically evaluated as:

$$\zeta_k = \frac{\delta_k}{\sqrt{4\pi^2 + \delta_k^2}} \tag{24}$$

Then, knowing the estimated modal damping ratio $\zeta_k$ and the estimated damped frequencies, the undamped natural frequencies can be obtained [3], [5]. The procedure described above derives from classical EFDD algorithms [5], [8], but it considers here a refined, computationally-efficient procedure with integrated double loop, that reduces possible bias errors and improves the achieved estimates.

## 3 Strong ground motions taken as base excitation

A series of multi-storey shear-type frames with different structural features has been analyzed [5]. From direct modal analysis, the modal parameters are determined before identification. Modal damping ratios are taken from 1% to 5% and up (till 10% in some cases). Results are available for two-, three- and six-storey frames; in the present work, only results for six-storey frames are reported for the sake of representation. The numerical input for the FDD algorithm is obtained by pseudo-experimental signals, generated prior to the dynamic identification. For all the examined cases, the structural response is solved by direct integration with Newmark's (average acceleration) method. Then, the simulated responses (storey accelerations) are used as input channels for the application of the refined FDD algorithm.

In view of assessing the algorithm's efficiency, a series of random noise excitations is adopted first as base excitation of the frames. Also, high damping ratios are concomitantly adopted at this stage. The estimated results turn-out very good for all the modal parameters of the structure, see [5], [6].

Then, the algorithm's efficiency is further assessed through a set of strong motion records, taken as shaking at the base of the structures [5]. Here, the analysis is widely extended with various seismic excitations and structures at variable damping ratios. Frames are subjected, into the present work, to a set of eight strong ground motions. In the present reference order:

- L'Aquila Earthquake - **AQ** (Abruzzo, Italy, 6 April 2009): M = 5.8, AQV Station - WE component, PGA = 646.1 cm/s$^2$ = 0.659 g;
- Maule Earthquake - **CH** (Maule, Chile, 27 February 2010): M = 8.8, Angle S/N 760 Station - WE component, PGA = 306.9 cm/s$^2$ = 0.313 g;
- El Centro Earthquake - **EC** (Imperial Valley, California, 8 May 1940): M = 7.1, USGS-NSMP Station 0117 - NS component, PGA = 306.5 cm/s$^2$ = 0.312 g;
- Imperial Valley Earthquake - **IV** (Imperial Valley, California, 15 October 1979): M = 6.4, CGS-CSMIP Station 01260 - NS component, PGA = 531.3 cm/s$^2$ = 0.542 g;
- Loma Prieta Earthquake - **LP** (Santa Cruz Mountains, California, 17 October 1989): M = 7.1, CGS-CSMIP Station 47459 - WE component, PGA = 352.3 cm/s$^2$ = 0.359 g;
- Christchurch Earthquake - **NZ** (Christchurch, New Zealand, 3 September 2010): M = 7.1, GDLC-GNS Station 163541 - NS component, PGA = 737.7 cm/s$^2$ = 0.752 g;
- Northridge Earthquake - **NO** (San Fernando Valley, California, 17 January 1994): M = 6.7, CGS-CSMIP Station 24436 - WE component, PGA = 1744.5 cm/s$^2$ = 1.778 g;
- Tohoku Earthquake - **TO** (Miyagi, Japan, 11 March 2011): M = 9.0, MYG004 Station - NS component, PGA = 2647.8 cm/s$^2$ = 2.699 g.

These eight seismic excitations are characterized by different frequency content, generally acting in a narrow time window, jointly with a high energy content, and shall be representative of a wide variety of earthquakes. In following Fig. 3, Frequency/Time Spectrograms related to each adopted seismic excitation are represented, with the purpose to inspect their characteristics, i.e. their frequency content and related power for every time and frequency instance. The limit of the time axis (x) is the length of the recording, while the limit of the frequency axis (y) is related to the so-called Nyquist frequency of the signal, namely half of the sampling frequency adopted by the acquisition system. The color scale represents the power of the signal, in terms of spectrum ($[(m/s^2)^2/Hz]$). The colormap is set from deep blue to bright red, from the lowest to the highest power. The differences between the eight excitations and with the canonical white noise input excitation, which is characterized by a uniform spectrum in frequency content for every time instant, are highlighted. On the contrary, strong motion data that are considered in this work are characterized by very short, non-stationary records and non-homogeneous frequency spectra. These features may affect the modal response and may lead to challenging estimates of the modal parameters [5], [6], [10], [11]. Anyway, the developed algorithm, with its refined computational strategies, leads to very good estimates of the modal parameters, as represented in following Section 4. The present study on the spectrograms should also help in understanding why eventually some earthquakes may lead to very accurate results, while others may lead to less effective outcomes, though estimates shall be conceived as quite good overall.

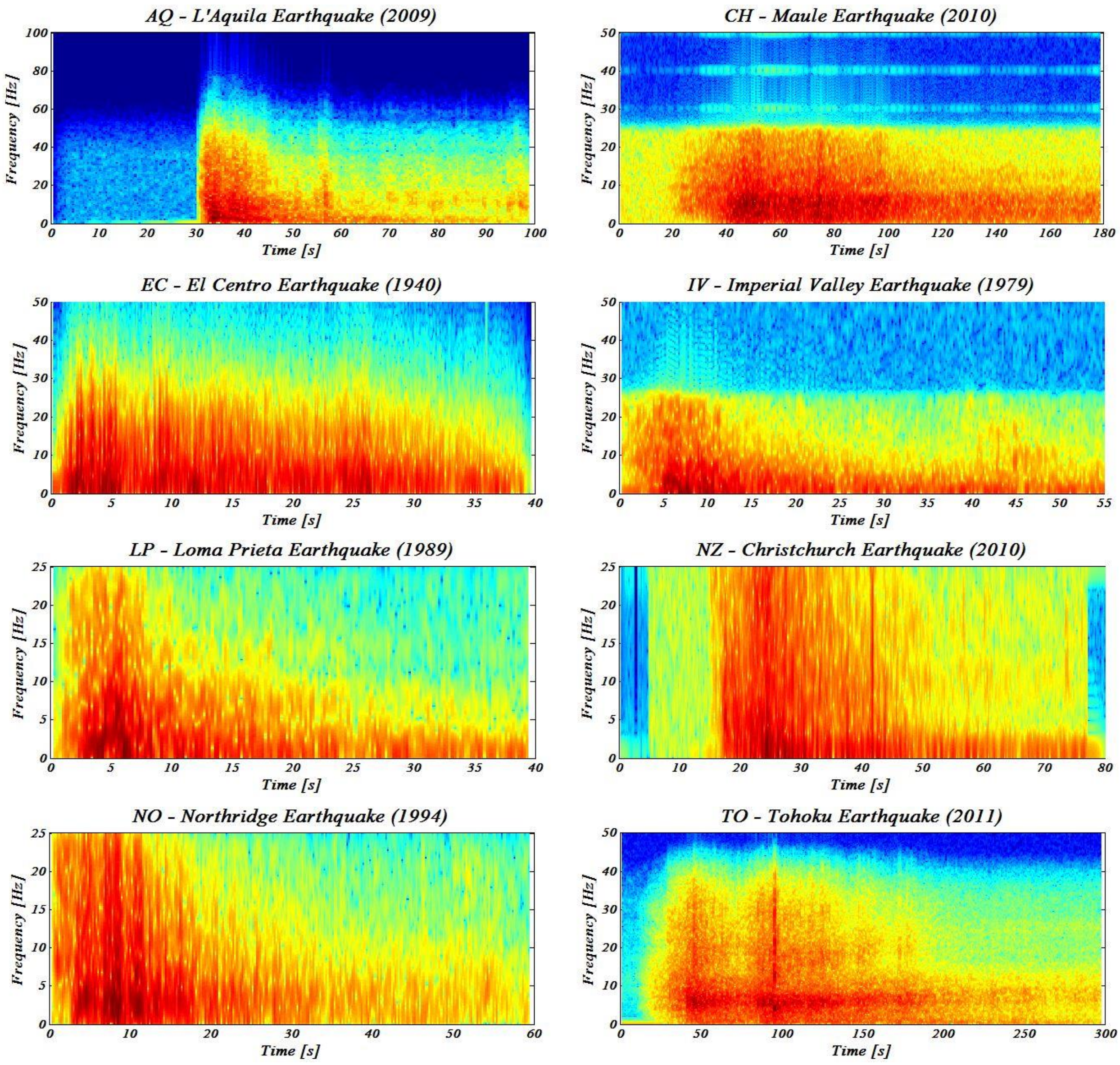


Figure 3: Frequency/Time Spectrograms of the set of adopted strong ground motion input data.

# 4 FDD modal dynamic identification based on seismic input

The present refined FDD algorithm is assessed by trials with the set of eight adopted seismic input signals. In this section, results for a six-storey frame, characterized by modal damping ratios $\zeta_k = 1\%$ for all the modes are reported. Also cases with $\zeta_k = 3\%$ and $\zeta_k = 5\%$ have been treated, but are not shown in the present paper, due to lack of room. Despite seismic input characteristics, all structural modes are excited enough to be identified all, through their resonance peaks, into the first singular value of the SVD. Previous Figs. 1a,b have shown a clear example. The PSD matrix is always estimated by the use of the Welch Modified Periodogram [14], opportunely set; the use of the standard procedure, though producing less accurate results, shall lead to substantial help in the location of the correct resonance peaks [12]. With this procedure, the estimate of modal parameters is feasible by operating on different SVs at the same time [5]: an example is shown in following Fig. 4a, where the SVD of the PSD matrix is represented.

The PSD matrix, computed at each frequency line of the spectrum, fulfills all the properties required for the correct working of the FDD technique, i.e. real diagonal terms and complex conjugate off-diagonal entries, leading to a hermitian PSD matrix. Accordingly, the related phase angles are always zero on the diagonal and display a 180° shift outside. An example of this fundamental feature is clearly observable in following Figs. 5 and 6, where examples of PSD matrix magnitudes and phase angles are shown.

The filtering of data before the modal identification (i.e. filtering of the simulated responses adopted then as input channels for the refined FDD algorithm) is necessary to leave-out undesired frequency contents, that for the civil structures correspond to the high frequency components of the spectra. This portion of the spectra may be significant with earthquakes, and might be reduced or removed by an adequate low-pass filtering of the acquisitions. Estimates take quite a significant advantage from this feature [12]. Also, the other procedures related to the refined FDD algorithm reported in Sections 2.1 and 2.2 help in improving the achieved estimates of the modal parameters, by truly allowing to apply the FDD identification technique on earthquake output signals, at least for pseudo-experimental signals. Analyses with real signals are currently under target with the use of the present refined FDD algorithm and seem promising in terms of good estimates of the modal parameters [7], [12].

In case of very noisy SVs (e.g. especially with high modal damping ratios), it is also possible to use appropriate computational strategies, associated to the standard procedure for the computation of the SVD: in this case, with respect to the use of the classical Welch's procedure, it is possible to operate on different SVs at the same time, as it is represented in Fig. 4a, to obtain very reliable estimates of the modal damping ratios [5], [6]. In such a way, a partial overlapping of SVs is possible: the individuation of spectral bells can be originally made as a composition of portions of different SVs, similarly to what done in the common technique, deriving from EMA's strategies, named overlapping [2], [6]. So, a fictitious SDOF SV can be built, and this substantially helps in the estimates of the damping ratio; further details on this feature may be found in [5], [6]. An example is reported in following Fig. 4b, where the spectral bell related to the fourth mode of vibration is composed as a fictitious SV from portions of different SVs (in this case the I, II, III and IV modes are adopted).

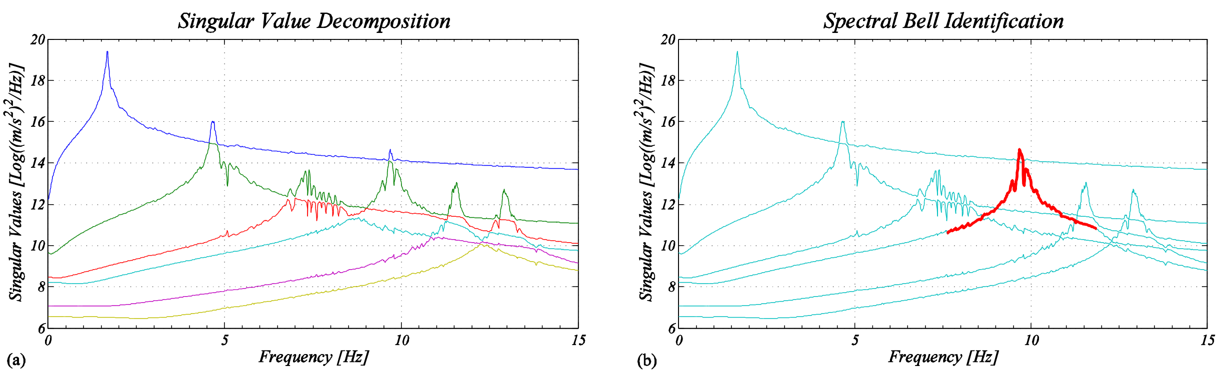


Figure 4: Display of the SVD obtained by a standard PSD matrix evaluation procedure and spectral bell identification of the fourth mode by a fictitious SV; six-storey frame, L'Aquila earthquake.

The frequency resolution adopted for the PSD matrix evaluation is another fundamental issue towards achieving reliable modal parameter estimates, especially for the damping ratios. This looks an essential feature for the use of the seismic input, that for its intrinsic short duration may affect the frequency resolution, which may result very poor and then significantly influence the estimates. In the literature, it is generally said that registration lengths of about 1000-2000 times the first natural period often result to be quite appropriate [1]. This operation was briefly explained in previous Section 2.2.1; more specifications can be found in [4], [5], where some case studies relating the record length to the estimates of the modal parameters are considered.

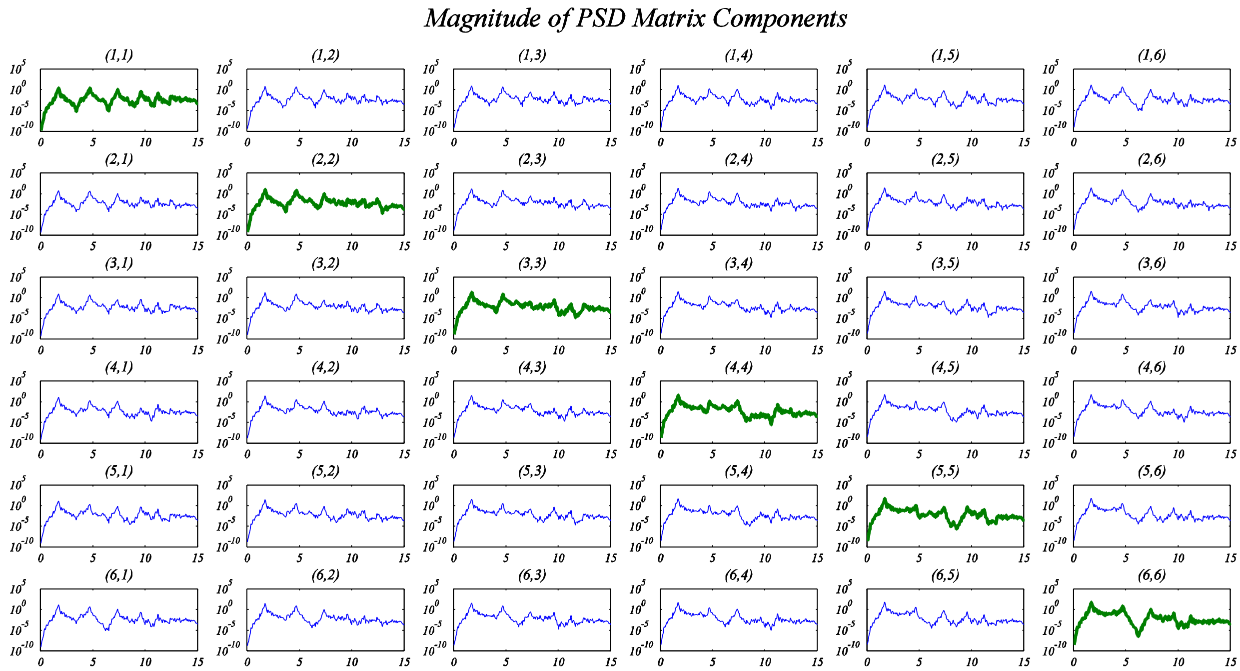


Figure 5: Magnitude of the (6×6) PSD matrix components computed at each frequency line [Hz], six-storey frame, El Centro earthquake.

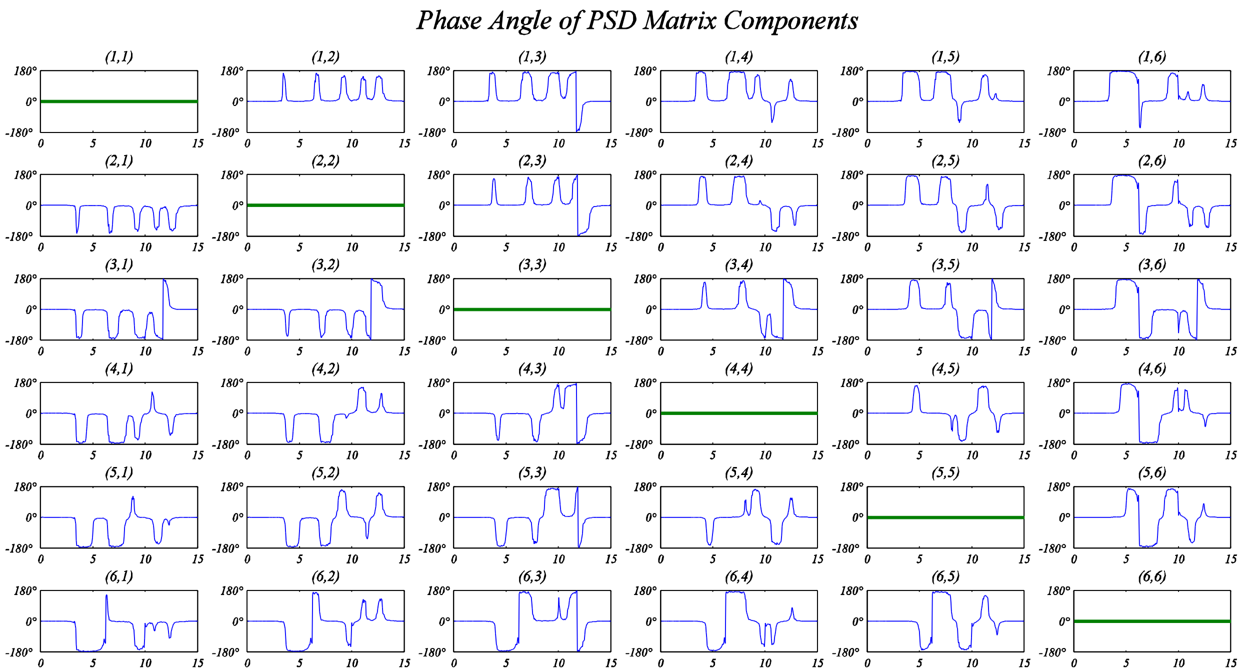


Figure 6: Phase angle of the (6×6) PSD matrix components computed at each frequency line [Hz], six-storey frame, El Centro earthquake.

The set of eight earthquake excitations at the base was used for the analysis of all the shear-type frames, with varying modal damping ratios for the vibration modes. The efficiency of the algorithm with seismic input is verified, demonstrating very good estimates for all the modal parameters of the structure. In particular, the mode shape estimates are very accurate: following Fig. 7 represents an example of the identified mode shapes for a case characterized by $\zeta_k$ = 1% and El Centro seismic input.

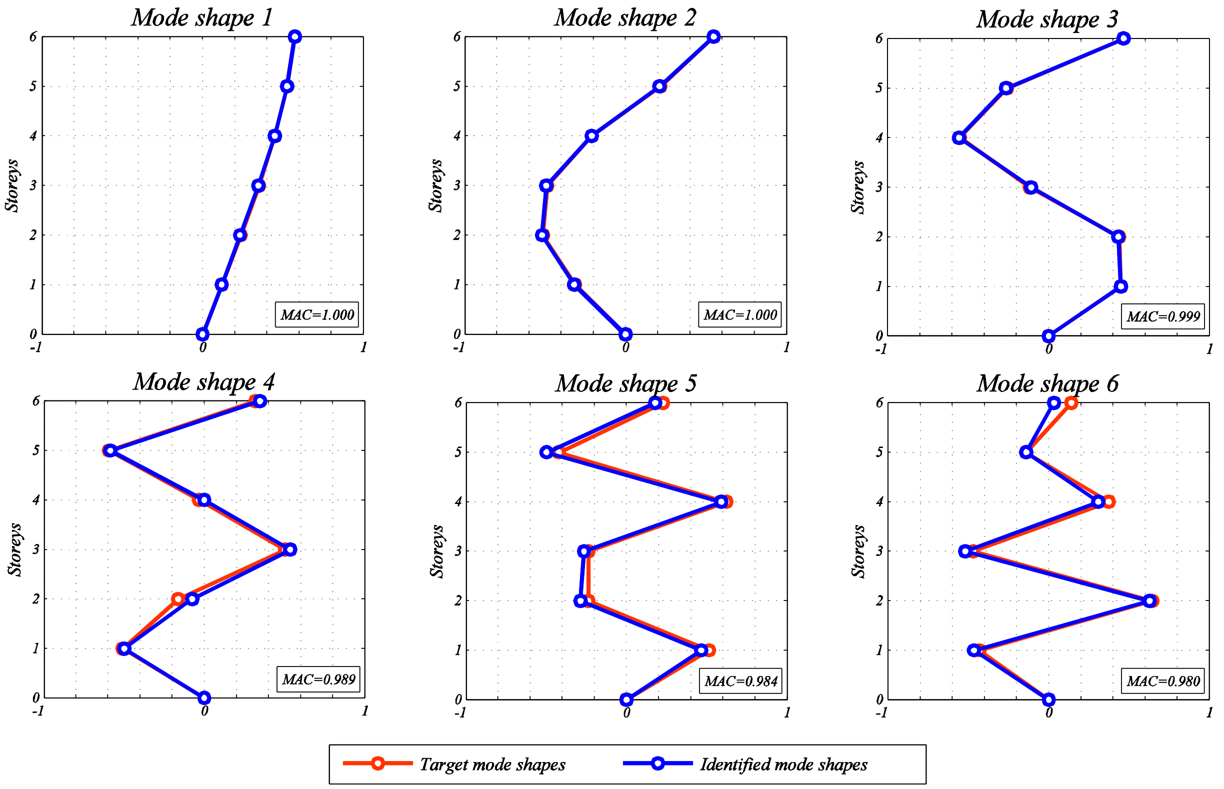


Figure 7: Example of estimated mode shapes for a six-storey frame, El Centro earthquake.

Subsequent Fig. 8 represents, for the same case, the associated MAC, Auto-MAC and Auto-MPC indices. The MAC index represents the correlation between the k$^{th}$ estimated mode shape $\phi_{k,est}$ and the related targeted mode shape $\phi_{k,tar}$, i.e. MAC = MAC($\phi_{k,est}$, $\phi_{k,tar}$), as outlined in previous Section 2.2. The Auto-Modal Assurance Criterion (Auto-MAC) index is a version of the MAC in which the estimated mode shapes are correlated with themselves, Auto-MAC = MAC($\phi_{k,est}$, $\phi_{j,est}$); it is useful to detect if some modes are not orthogonal to each-other. This index helps with modal identification when no target parameters are available for comparison purposes [10]: indeed, all diagonal terms are unitary by definition, while off-diagonal terms, due to the orthogonality hypothesis between the modes, shall be at around zero.

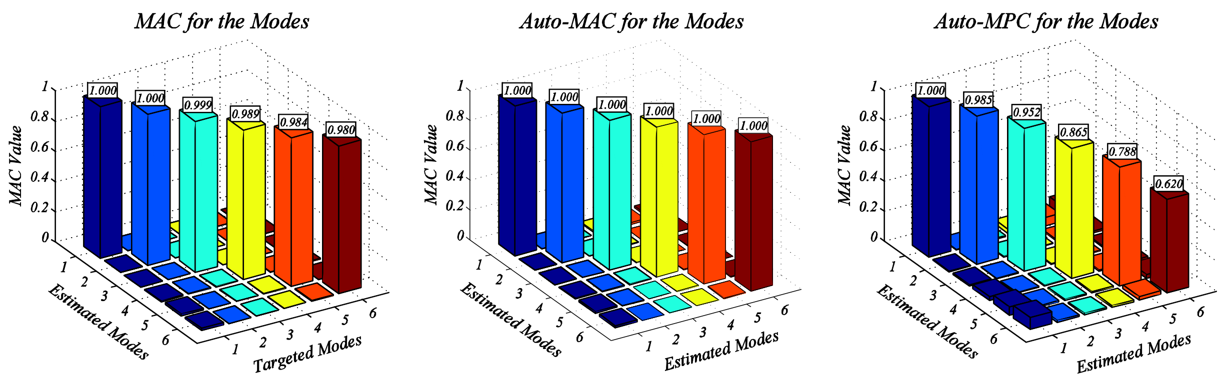


Figure 8: Modal Assurance Criterion, Auto-Modal Assurance Criterion and Auto-Modal Phase Collinearity for the estimated mode shapes; six-storey frame, El Centro earthquake.

The existence of non-zero off-diagonal terms indicates little degree of correlation between some of the modes, i.e. some of them are not correctly estimated (or in some cases estimates are not reliable). Finally, the Auto-Mode Phase Collinearity (Auto-MPC) is an index that checks the degree of complexity of a mode, i.e. it evaluates the functional linear relation between imaginary and real parts of the mode shape components [10]. This index is based on variance-covariance matrix computations applied to the estimated mode shapes, and can be calculated as the MAC index among an estimated mode shape and its complex conjugate, Auto-MPC = MAC($\phi_{k,est}$, $\overline{\phi}_{j,est}$). An MPC index greater than, say, 0.5 may be interpreted as if the mode shape vector components are all in-phase (and then the estimates are considered to be suitable), while a lower value suggests anomalous fluctuations of the phases. Also, a visual inspection is possible at this stage [10]. As for the Auto-MAC, the off-diagonal Auto-MPC terms must be approximately zero: as previously, the existence of non-zero off-diagonal terms checks if some modes may not be successfully estimated, and shall help with the modal parameter identification [10].

For all the cases, the obtained results are very much consistent with the target values, as it is possible to be seen in Figs. 9 and 10, where the estimates obtained through the present refined FDD algorithm at seismic input are shown in the form of bar charts for all the set of ground motions. These figures also belong to the identification applied to the six-storey shear-type frame with $\zeta_k$= 1%, where higher effectiveness at low damping is expected and actually recorded.

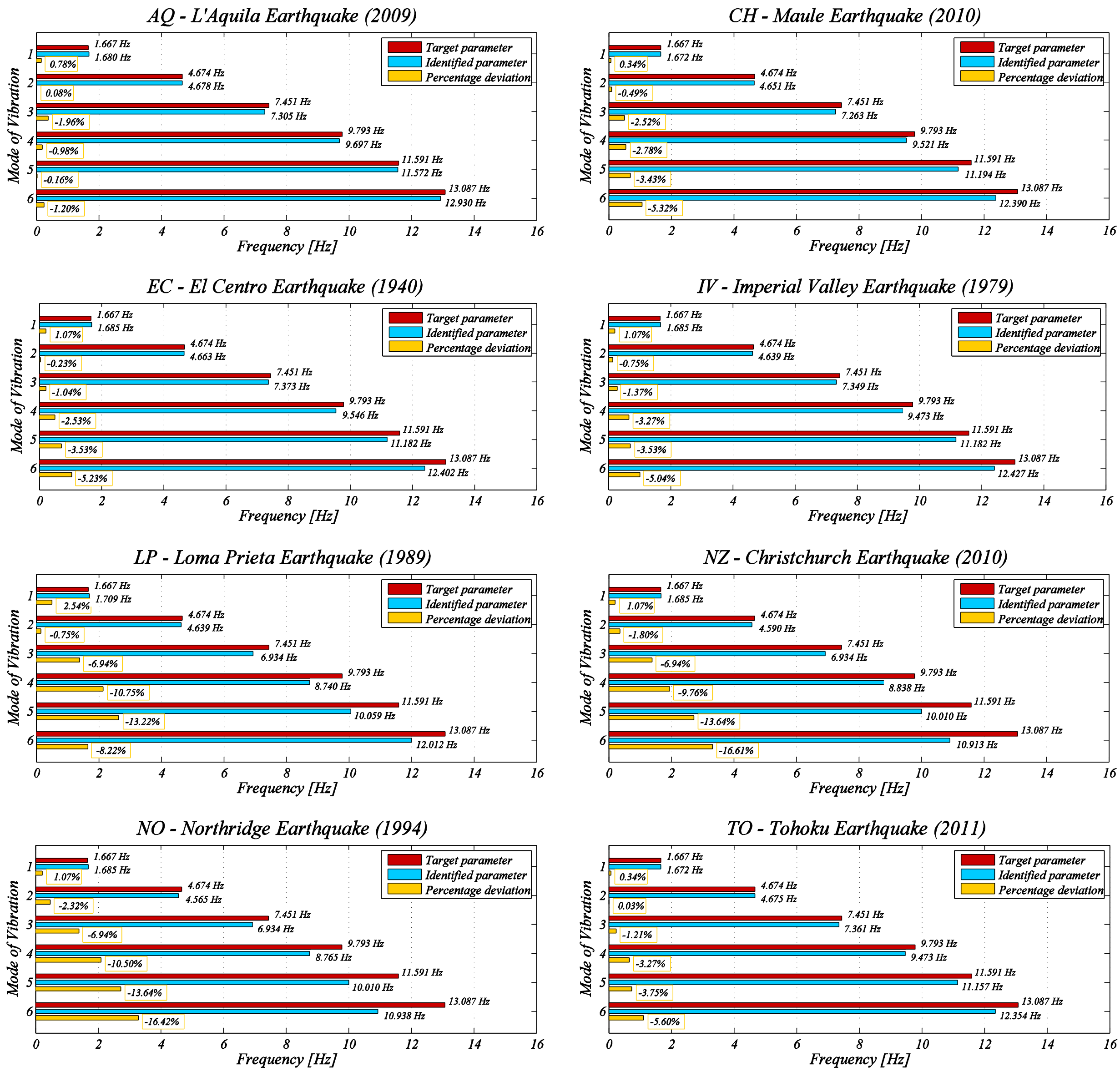


Figure 9: Estimated natural frequencies for the set of considered strong ground motions, six-storey frame.

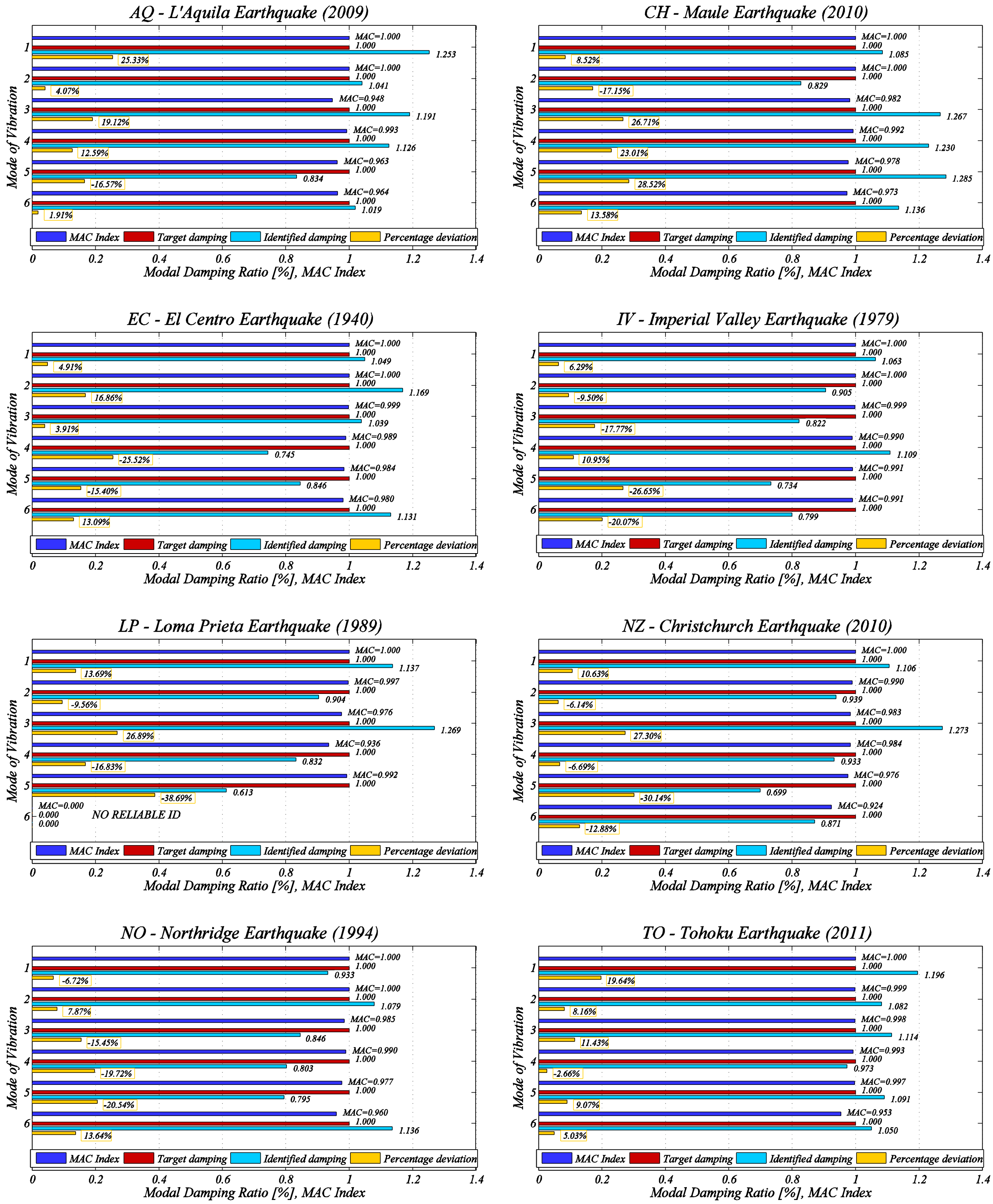


Figure 10: Estimated mode shapes (MAC index) and modal damping ratios [%] for the set of considered strong ground motions, six-storey frame.

In particular, for $\zeta_k = 1\%$, the natural frequencies display deviations that are less than 5% on average; especially on the first three to four modes of vibration, the estimates look very accurate. The last three modes for the LP, NZ and NO cases are affected by slight more deviations: this is due to the particular frequency content of these three seismic excitations (Fig. 3), jointly with the poor resolution of the recordings (the Nyquist frequency is only 25 Hz). This probably adversely affects the estimates. Mode shape estimates are always very accurate, with MAC values always over 0.90. Only the last mode of vibration of the LP case is missing. This is also suggested from the results belonging to the Auto-MAC and Auto-MPC computations, which report anomalous values related to the sixth mode of vibration. It is significant to emphasize that these tools are crucial also in cases where no target parameters are known, helping for the correct individuation and choice of the modal peaks, and then for assessing the consistency of the modal parameter estimates. Further, damping ratios are correctly estimated, with slight deviations (always below 30%, and on 10÷15% on average).

The estimates for the cases characterized by higher modal damping ratios of 3% and 5% are a little less accurate, but the results are in any case sufficiently good. Natural frequencies are correctly estimated, with deviations in the order of less than 10% on average. Mode shapes estimates have MAC index around 0.9 for the first four modes, for $\zeta_k = 3\%$, and for the first three modes, for $\zeta_k = 5\%$. The identification basically fails for the subsequent modes: this is reported also by erroneous values of the Auto-MAC and Auto-MPC indices. These failures shall not matter much in engineering terms, because of the very little modal participating mass related to these modes for the considered frames. In fact, the first three modes of vibration are truly representing the seismic dynamic response of the structures under target and then they are consistently captured. Finally, damping ratios are estimated appropriately for all the identified modes, by showing an average deviation that is reasonably contained, say less than 30% in all cases, on average.

# 5 Conclusions

This research work has proposed an implementation of a refined Frequency Domain Decomposition algorithm in order to achieve effective estimates of all the structural modal parameters, i.e. natural frequencies, mode shapes and damping ratios. This method shall identify the dynamic properties of the structures from their recorded responses, with unknown input, as OMA techniques require. Comparing to currently-available techniques in the frequency domain, especially classical FDD algorithms (which can be effectively used only with stationary Gaussian white noise input data and weakly-damped structures), the proposed refined FDD algorithm looks able to extract very reliable modal parameter estimates, by adopting earthquake response excitations as input for the identification procedure, including for strong motion records. Also, concomitant high values of modal damping are effectively targeted.

First, canonical force input based on random noise force was adopted on different shear-type frame structures, with the purpose to assess the procedure within typical hypotheses of FDD validity. Then, modal identification has been successfully attempted at seismic input, taken as ground excitation at the base of the same frames. A set of eight strong ground motions with different characteristics (i.e. frequency sampling, duration, frequency content, power, etc.) has been employed. At this stage, only results for six-storey frames with $\zeta_k = 1\%$ for all the modes have been exposed: for these cases, estimates are strongly consistent with target values, despite leaving typical working hypotheses of the FDD procedures. Anyway, all the examined cases exhibited very consistent results, in particular for the estimates of the natural frequencies, that are assessed with quite high accuracy. Only the last modes related to three earthquake instances are affected by slight deviations. Also, the other modal parameters are estimated with quite limited errors, and this holds true as well for quite high damping ratios. In fact, also for cases characterized by $\zeta_k = 3\%$ and $\zeta_k = 5\%$ estimates turn-out very reliable in engineering terms, especially for the natural frequencies.

Investigations and original implementations about the processing of the PSD matrix, the use of untrended auto- and cross-correlations, the importance of frequency resolution and of the prior filtering of data, the use of MAC, Auto-MAC and Auto-MPC indices are thoroughly inspected, to reach reliable estimates of the modal parameters at seismic input. Moreover, careful treatments of spectral bell width, singular value and peak selection (even with distinct or overlapping SVs), and regression time window have been located as crucial issues towards reaching valuable estimates of the modal damping ratios. Thus, the attempted simulations with pseudo-experimental signals shall confirm the efficacy of the implemented algorithm, together with the possibility to perform FDD identification on earthquake output signals. It is shown that, in principle, FDD dynamic identification of structural modal properties of frames at seismic input shall be possible, with potential implications in the general realm of structural dynamics and, possibly, in the specific field of earthquake engineering. Trials with real earthquake signals are currently under target.

## Acknowledgements

The Authors would like to acknowledge public research funding from *"Fondi di Ricerca d'Ateneo ex 60%"* and a ministerial doctoral grant and funds at the ISA Doctoral School, University of Bergamo, Department of Engineering (Dalmine).


## References


[1] E. Reynders, *System identification methods for (Operational) Modal Analysis: review and comparison*, Archives of Computational Methods in Engineering, Vol. 19, No. 1, Springer, pp. 51-124, 2012.

[2] M. Maia, M. Silva, *Theoretical and Experimental Modal Analysis*, Research Studies Press LTD, Taunton, England, 1997.

[3] R. Brincker, L. Zhang, P. Andersen, *Modal identification of output-only systems using frequency domain decomposition*, Smart Materials and Structures, Vol. 10, No. 3, IOP Publishing, pp. 441-445, 2001.

[4] F. Pioldi, *Sulla stima dello smorzamento modale mediante algoritmo Frequency Domain Decomposition*, B.Sc. Thesis in Building Engineering, Advisor E. Rizzi, Università di Bergamo, Dipartimento di Ingegneria, pp. 169, February 2012.

[5] F. Pioldi, *Sulla formulazione di algoritmi ottimizzati di identificazione dinamica modale e loro applicazione in ambito sismico*, M.Sc. Thesis in Building Engineering, Advisor E. Rizzi, Università di Bergamo, Dipartimento di Ingegneria, pp. 359, December 2013.

[6] F. Pioldi, R. Ferrari, E. Rizzi, *Output-only modal dynamic identification of frames by a refined FDD algorithm at seismic input and high damping*, Submitted for publication, November 2013.

[7] F. Pioldi, R. Ferrari, E. Rizzi, *Operational Modal Analysis of structures under real strong motion recordings by a refined FDD algorithm*, In preparation, 2014.

[8] R. Brincker, C. Ventura, P. Andersen, *Damping estimation by Frequency Domain Decomposition*, in A.L. Wicks, R. Singhal, Editors, *Proceedings of the 19th International Modal Analysis Conference (IMAC19), Hyatt Orlando, Kissimmee, Florida, February 5-8, 2001*, Society for Experimental Mechanics, pp. 698-703, 2001.

[9] R. Brincker, L. Zhang, *Frequency Domain Decomposition revisited*, in C. Gentile, F. Benedettini, R. Brincker, N. Møller, Editors, *Proceedings of the 3rd International Operational Modal Analysis Conference (IOMAC), Portonovo (Ancona), Italy, May 4-6, 2009*, Starrylink, pp. 615-626, 2009.

[10] S. Ghahari, F. Abazarsa, M. Ghannad, E. Taciroglu, *Response-only modal identification of structures using strong motion data*, Earthquake Engineering and Structural Dynamics, Vol. 42, No. 11, Wiley, pp. 1221-1242, 2013.

[11] C.E. Ventura, R. Brincker, P. Andersen, *Dynamic Properties of the Painter Street Overpass at Different Levels of Vibration*, in C. Soize, G.I. Schuëller, Editors, *Proceedings of the 6th International Conference on Structural Dynamics (EURODYN), Paris, France, September 4-7, 2005*, Millpress, pp. 167-172, 2005.

[12] F. Pioldi, E. Rizzi, *On the analytical formulation and implementation of Frequency Domain Decomposition algorithms for Operational Modal Analysis*, Technical Report, Università di Bergamo, Dipartimento di Ingegneria, In preparation, 2014.

[13] J. Bendat, A. Piersol, *Random Data, Analysis and Measurements Procedures*, Wiley, New York, 1986.

[14] P.D. Welch, *The use of Fast Fourier Transform for the estimation of Power Spectra: a method based on time averaging over short, modified periodograms*, IEEE Transactions on Audio and Electroacoustics, Vol. 15, No. 2, IEEE Publications, pp. 70-73, 1967.